

We are IntechOpen, the world's leading publisher of Open Access books Built by scientists, for scientists

6,900

Open access books available

186,000

International authors and editors

200M

Downloads

Our authors are among the

154

Countries delivered to

TOP 1%

most cited scientists

12.2%

Contributors from top 500 universities



WEB OF SCIENCE™

Selection of our books indexed in the Book Citation Index
in Web of Science™ Core Collection (BKCI)

Interested in publishing with us?
Contact book.department@intechopen.com

Numbers displayed above are based on latest data collected.
For more information visit www.intechopen.com



Transmission of CO₂ Laser Radiation Through Glass Hollow Core Microstructured Fibers

A. D. Pryamikov, A. F. Kosolapov, V. G. Plotnichenko and E. M. Dianov
*Fiber Optics Research Center of Russian Academy of Sciences
Russian Federation*

1. Introduction

In this chapter we would like to highlight and analyze the main problems of transmission and propagation of CO₂ laser radiation in the hollow core microstructured fibers (HC MFs). It is well known that there is a strong need for the fiber delivery systems for 10.6 μm CO₂ lasers due to a wide range of CO₂ laser applications in medicine, spectrometry, industry, military applications and in other fields of science and technology. Research into the possibility of the mid IR laser radiation transmission (especially, CO and CO₂ lasers) with the help of optical fibers as well as with crystalline or glass cores made of different materials has been going hand with hand with the technological development. However, until recently these fibers haven't been used for industrial applications due to a relatively high level of optical losses at the lasers wavelengths and certain physicochemical properties of the fiber materials. These problems mainly arise from a low laser damage threshold, low melting temperatures of most IR transmitting materials and their high nonlinearity.

Hollow waveguides are exempt from many problems that are common to all types of the solid waveguides in this spectral region and thus can serve as much more reliable delivery systems. Glass hollow waveguides, crystalline hollow waveguides, dielectric - coated cylindrical hollow waveguides, polycrystalline fibers are well known examples of such systems. Here we consider only the glass HC MFs with their characteristics and physical phenomena laying the basis for their waveguide mechanisms. In particular, we propose a new type of HC MF for CO₂ laser radiation delivery with the cladding consisting of one row of the glass capillaries. We show that due to complicated boundary conditions and optical properties of an individual capillary it is possible to obtain low loss waveguide regimes for CO₂ laser radiation. Moreover, we show that the HC MFs with a determined symmetry type of a capillary arrangement in the cladding exhibit low bend losses when such low loss waveguide regimes occur.

The chapter is organized as follows. In Section 2 we consider all types of proposed hollow waveguides for CO₂ laser radiation transmission and give a short historical overview to highlight the problem of CO₂ laser beam delivery in the hollow core waveguides. In Section 3 we consider physical mechanisms of the light guiding in the glass HC MFs with cladding consisting of capillaries due to which, in our opinion, it becomes possible to guide the light in the mid IR including CO₂ laser radiation. In Section 4 we offer some numerical analyses

and show a possibility to achieve low loss waveguide regimes in such HC MFs by careful selection of geometry parameters characterizing the fibers and a glass refractive index. Section 5 contains conclusions.

2. CO₂ laser radiation transmission through hollow core waveguides

A variety of waveguides has been studied for the delivery of CO₂ laser energy. In this section we consider briefly all types and properties of hollow waveguides and HC MFs for the CO₂ laser radiation transmission known up to now.

2.1 Historical overview of CO₂ laser radiation transmission through hollow waveguides

Rectangular core hollow waveguide structures were the first suggested for the delivery of CO₂ laser radiation [Nishihara et. al., 1974]. The first publication on the IR spectral transmission measurements of a rectangular hollow waveguide dates back to [Garmire, 1976]. The hollow waveguide described was made of aluminium strips with heights greater than 0.5 mm demonstrating a delivery over 200 W of continuous CO₂ laser radiation with no damage to the structure [Garmire et. al., 1979]. However, such metallic rectangular waveguides are not suitable for many practical applications due to their relatively big outer dimensions $\sim 1 \text{ mm} \times 10 \text{ mm}$ in cross section while smaller dimensions made the loss was too high for any practical use. Thus the search for materials and waveguides more suitable for practical applications continued and, a few years later, in [Laakmann, 1987] there was proposed a way to decrease the outside dimensions of HC waveguides to under 2 mm in diameter and to increase the reflectivity of the bore inside surface. Silver was used as a substrate metallic material of the rectangular core on which several dielectric coatings were deposited. By doing so, the author succeeded in maintaining a practical transmission level for the hollow rectangular waveguides. However, as imperfections of the inside geometry and surfaces affected the transmission, the design of the rectangular hollow waveguide proposed in [Laakmann, 1987] had to be improved [Mashida et. al., 1991]. The authors proposed a hollow waveguide having the same cross section design as in [Laakmann, 1987] but with multiple dielectric coatings on the inside surfaces to increase its reflectivity. As a result, 1 - mm - core straight rectangular hollow waveguide of such construction had a loss $\sim 0.1 \text{ dB/m}$ for circularly polarized CO₂ laser radiation. Moreover, the waveguide demonstrated the low loss for a bend. The next attempt to decrease loss for the rectangular core hollow waveguides was described in [Karasawa et. al., 1990]. The authors proposed and fabricated a germanium coated rectangular hollow waveguide with a cross section of 2 mm², a length of 80 cm and a loss of less than 0.1 dB/m was fabricated. The resulting waveguide had a relatively low loss even for a bend.

However, the main disadvantage of the rectangular hollow waveguides is their relatively large outer dimensions and low flexibility which has led to a greater popularity of circular hollow waveguides. These waveguides made of glass, metal or plastic are those most commonly used today. Along general lines, circular cross section hollow waveguides for CO₂ laser radiation transmission can be divided into two groups: attenuating total reflecting and leaky waveguides. The metallic or dielectric films are deposited on the inside of metallic, plastic or glass tubing. Attenuating total reflecting hollow waveguides have inner

core materials with a refractive index less than 1. Due to this fact, the angle of incident radiation in the core is greater than the critical angle and the light experiences the total internal reflection. An example of such fiber operating at the CO₂ laser wavelength is the sapphire fiber with a refractive index of $n = 0.67$ [Harrington & Gregory, 1990].

For our part, in the following subsections we will consider the second group of the circular cross section hollow waveguides, previously classified as leaky waveguides, in particular, HC MFs. This group of hollow waveguides has inner wall surface with refractive indices greater than 1. Leaky hollow waveguides have metallic or dielectric layers deposited on the inside metallic, plastic or glass tubing to enhance their surface reflectivity. Creation of such dielectric coated cylindrical hollow waveguides presented a complicated technological problem since high quality reflective coatings are not compatible with circular cross section geometry. Traditional vapor deposition techniques don't produce good quality coatings on the inside of a capillary. The theoretical calculated attenuation of a dielectric coated hollow waveguide for the IR region was obtained in [Miyagi & Kawakami, 1984]. The authors have shown that the attenuation is very sensitive to the material and geometry of a dielectric film. Also, the attenuation is very sensitive to the properties of the metal under the dielectric film. A metal should have a low refractive index and a very high extinction coefficient. For example, these can be silver, nickel, copper. A dielectric should be selected with a maximum refractive index, for example, KCl, ZnSe, ZnS etc. The first demonstration of a dielectric coated cylindrical hollow waveguide was performed by Prof. Miyagi's group [Miyagi et al., 1983] in 1983. The 1.2 m - long mandrel of polished aluminum tubing was coated with approximately 0.45 μm of germanium. Then, a layer of nickel up to 200 μm was deposited on the top of germanium before the aluminum mandrel was removed by leaching. The final structure was a nickel tube with optically thick dielectric layers on the inner wall. The fabricated waveguide had a core diameter of 1.5 mm and length of about 1 m. The measured attenuation was ~ 0.4 dB/m in the straight waveguide but the bend loss was very high.

Authors in [Croitoru et. al., U.S. Patent, 1990] have used polyethylene and Teflon tubing as a substrate in which thin and flexible metallic layers of Al followed by AgI were deposited. They reported attenuation in a straight waveguide of about 0.6 dB/m at the bore size value of 4 mm [Croitoru et. al., 1990]. Authors of [Morrow & Gu, 1994] reported a cylindrical hollow waveguide in which Ag and Ag halide coatings were deposited inside Ag tubes. The waveguide with 1 - mm - bore size had attenuation below 0.1 dB/m at $\lambda = 10.6$ μm which was still below 0.8 dB/m at a bend radius up to 25 cm.

At the end of this subsection, we will turn to the currently most popular hollow circular cross section waveguides for CO₂ laser radiation transmission. These are hollow glass waveguides developed initially by Prof. Harrington's group [Abel et. al., 1994]. There are two main advantages of the glass tubing substrate. First, it is easier to make a long, uniform tubing from glass having considerably smoother wall surfaces than metal or plastic tubings. As a result, the scattered losses are less. The second advantage is that the technology of making glass capillary tubings is common and inexpensive. The authors fabricated a hollow glass waveguide using wet chemistry methods. First, an Ag layer was deposited on the inside of a silica glass tubing. Then, an AgI layer was formed over the metallic film. The thickness of the layer was optimized to obtain a high reflectivity at the required wavelength. A straight waveguide with a bore of 530 μm demonstrated a loss of 0.3 dB/m at CO₂ laser wavelength. This fiber could maintain a loss level under 2 dB/m at a bend radius as small as

5 cm. Hollow glass waveguides have been used successfully for a modest CO₂ laser power delivery below ~ 80 W. For the higher power delivery it is necessary to place a water – cooled jacket around the guides. The highest CO₂ laser power delivered through the water – cooled hollow glass waveguide with 700 μm bore was 1040 W [Nubling & Harrington, 1996]. This is comparable to CO₂ laser power delivered through the water – cooled hollow metallic waveguide with 1800 μm bore which was 2700 W [Hongo et. al., 1992].

2.2 CO₂ laser radiation transmission through hollow core microstructured fibers

In this subsection we will consider a new approach to solving the problem of the mid IR transmission (in particular, CO₂ laser radiation) through the glass hollow core microstructured fibers (HC MFs). The possibility of the light confinement in the air core of HC MFs with the cladding consisting of two dimensional periodic array of air holes was predicted by Russell at the beginning of 1990s and theoretically demonstrated by Birks et. al. [Birks et. al., 1995]. The most advanced HC MFs are hollow core photonic crystal fibers (HC PCFs). HC PCFs in turn can be divided into two main groups. The HC PCFs from the first group guide the light by virtue of photonic band gap (BG HC PCFs). The HC PCFs from the second group have no band gaps and guide the light due to an inhibited coupling between the core guided modes and modes associated with a cladding [Benabid et. al., 2002]. They are called inhibited coupling HC PCFs (IC HC PCFs). Both types of HC PCFs have the claddings with very little solid material, usually, with a filling fraction less than 10%.

The guidance mechanism for BG HC PCFs is based on the concept of ‘out of plane’ band gap. The microstructure of BG HC PCF cladding consists of air holes packed in a triangular arrangement. It gives rise to a full two dimensional photonic band gap [Birks et. al., 1995]. As a result, forbidden frequencies occur for optical waves whose wave vector (axial) component is not equal to zero. Such frequency ranges constitute bands. The first experimental demonstration of light transmission in the BG HC PCF was made in 1999 [Gegan et. al., 1999]. Up to now, considerable efforts have been put forth in experimental and theoretical studies of BG HC PCFs made of silica glass [Humbert et. al., 2004; Benabid et. al., 2004]. This special interest can be partly explained by a need to find a way of yielding a loss level less than 0.2 dB/km for telecommunication spectral region. So far, the BG HC PCFs loss was reduced only to 1.2 dB/km due to intrinsic roughness of the air – glass interfaces in the structure [Roberts, Couny et. al., 2005].

As it was mentioned above, BG HC PCFs made of silica glass have claddings with very little solid material. The bandgap located between 4th and 5th bands is used for guiding in HC PCFs with such high air – filling fraction ($\geq 80\%$) [Humbert et. al., 2004]. The number of each band is counted from the band with the largest value of the propagation constant of the air core mode. However, there is an important need for BG HC PCFs which can be used in the mid and far IR. BG HC PCF made of silica glass with a core diameter of 40 μm demonstrated single mode waveguide regime in a narrow transmission window near the wavelength of $\lambda = 3.14$ μm with an attenuation of ~ 2.6 dB/m [Shephard et. al., 2005]. But silica glass BG HC PCFs cannot be used for CO₂ laser radiation transmission due to a very high material loss of silica. Transmission of light in the mid IR region becomes possible with BG HC PCFs made of glasses which are transparent in this spectral region such as

chalcogenide glasses. These glasses are composed of the chalcogen elements Se and Te with an addition of such elements as Ge, As, Sb. The transparency windows of these glasses correspond approximately to the mid IR region 2 – 25 μm .

Modeling of BG HC PCFs made of nonsilica glasses was performed by a number of authors [Shaw et. al., 2003; Pottage et. al., 2003; Pearce et. al., 2005]. In this paper [Shaw et. al., 2003] BG HC PCFs made of As – S (refractive index ~ 2.4) and As – Se (refractive index ~ 2.8) were analyzed. It was shown that there exist several spectral regions with bandgaps for an air filling fraction $> 40\%$ in both As – S and As – Se BG HC PCFs. These BG HC PCFs have large bandgap widths at the air filling fraction of 45% to 60%. BG HC PCFs with high air filling fractions $> 80\%$ also exhibited large bandgap widths. In the author's opinion, all these results show a possibility of a light transmission in the mid IR using chalcogenide BG HC PCFs. The authors of [Pottage et. al., 2003] have carried out a numerical analyses of BG HC PCFs for a wide range of refractive indices from $n = 1.5$ to $n = 3.6$ and for different values of air filling fractions from 33% to 87%. They discovered a new type of the bandgap which was called type 2 bandgap at an air filling fraction $\sim 60\%$ for any glass index beyond 2. The results showed a possibility of obtaining a satisfactory guidance in such BG HC PCFs.

Another important aspect of the problem of the mid IR radiation transmission was discussed in [Pearce et. al., 2005]. Apart from a limitation to attaining a low loss guidance in BG HC PCFs connected with the intrinsic roughness of the air glass interfaces, there is another problem connected with an existence of surface guided modes that are trapped in the core surroundings. Experimental and theoretical studies [Smith et. al., 2003; Humbert et. al., 2004; West et. al., 2004; Saitoh et. al., 2004] carried out for silica BG HC PCFs have shown that the anticrossing between dispersion curves of the surface modes and the air core modes is the main factor leading to a transmission loss in BG HC PCFs. Several methods were proposed to suppress the surface modes. The first method is used to reduce the distortion of the core by including 'fingers' of glass [West et. al., 2004]. The second method is to use thin core walls [Saitoh et. al., 2004] and the third one is to use 'antiresonance' walls [Roberts, Williams et. al., 2005]. The authors of [Pearce et. al., 2005] modeled a realistic design of distorted cores for BG HC PCFs which can guide the light in the type 2 bandgap. They have demonstrated that BG HC PCFs made of high index glass can guide a fundamental air core mode with a fraction of power in the air of up to 98%.

In their paper [Hu & Menyuk, 2007] the authors analyzed BG HC PCFs for refractive indices between 1.4 and 2.8. They found two maxima of the relative bandgap as a function of the air filling fraction and refractive index. The authors also found that the relative bandgap and the level of loss are interrelated. When the relative bandgap increases the loss decreases and vice versa.

Despite the promising results of modeling obtained in the above listed works a practical realization of BG HC PCFs made completely of chalcogenide glass for the mid IR spectral region has not been reported. The only successful realization of a photonic band gap hollow core fiber for the CO₂ laser radiation transmission was 'Omniguide' fiber where the cladding is a Bragg reflector (hollow core Bragg fiber) made of soft glass and polymer [Temelkuran et. al., 2002]. The authors of [Bowden & Harrington, 2009] have studied low and high index chalcogenide glasses for their potential use in the fabrication of all glass hollow core Bragg fiber.

The first work devoted to the fabrication and experimental investigation of BG HC PCF for CO₂ laser radiation transmission has appeared only in 2010 [Deseveday et. al., 2010]. The authors designed BG HC PCF made of chalcogenide glass to guide the light in the air core at $\lambda = 9.3 \mu\text{m}$. They also fabricated two BG HC PCFs which could potentially guide CO₂ laser radiation but no guidance was observed. The authors explained this fact by technological difficulties in the fabrication process. They hope to improve the process by avoiding air tightness anomalies and by decreasing the core's wall thickness.

In the next section we will represent our approach to solving the problem of CO₂ laser radiation transmission through the glass HC MFs.

3. Mechanisms of CO₂ laser radiation transmission through the glass hollow core microstructured fiber with the cladding consisting of capillaries

In this section, we will consider physical mechanisms and principles which enable, in our opinion, to obtain a loss level much lower than the material loss of the glass of HC MFs with a negative curvature of the core boundary [Pryamikov et. al., 2011]. The negative curvature of the core boundary is obtained by the cladding consisting of one or several rows of glass capillaries. Such microstructure design leads to a significant complication of the boundary conditions for the air - core modes. To justify our assumptions it will be necessary to consider a plane wave scattering on a cylindrical surface to show an analogy between this phenomenon and the light scattering on the plane optical diffraction grating. An analogy between discrete rotational symmetry of the capillary arrangement in the cladding and the plane diffraction grating will also be outlined. We will also consider the second main factor leading to a loss reduction of the air core modes of the HC MFs and to an increase in the width of transmission regions. It is connected with the geometry parameters of an individual capillary and the glass refractive index. In the end, we will try to justify the statement how these factors can result in the loss reduction of the air core mode in HC MF with the cladding consisting of capillaries with respect to the BG HC PCFs and kagome lattice IC HC PCFs.

3.1 The cylindrical surface as a diffraction grating

In this subsection, we will offer a reason which, in our opinion, lies behind the low loss waveguide regimes for the glass HC MFs with negative curvature of the core boundary. For the first time, an effect of the loss level decrease resulting from the negative curvature of the core boundary was observed for a large pitch kagome - lattice IC HC PCF with a hypocycloid - shaped core structure (the second group of PCFs) [Wang et. al., 2011]. We have used a simple cladding structure of the HC MF consisting of eight silica capillaries (Fig. 1(left)). Such HC MF guided light in the mid IR up to 4 μm despite of very high material losses of silica in this spectral region. In this case, the negative curvature of the core boundary was created by the capillary surfaces. Of course, such long a wavelength guiding is determined by not only the negative curvature of the core boundary but (may be to a greater extent) also by the optical properties of an individual capillary of the cladding. For example, the simple cladding structure consisting of one row of the capillaries has a lower density of eigenstates with respect to the cladding consisting of the solid rods (Fig. 1(right)).

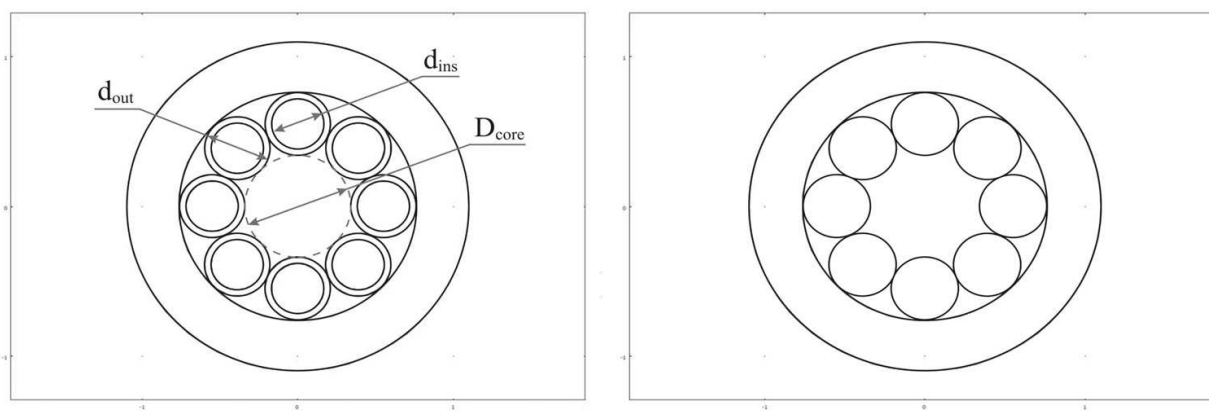


Fig. 1. (left) HC MF with the cladding consisting of eight capillaries (right) HC MF with the cladding consisting of eight solid rods.

In [Pryamikov et. al., 2011] the authors have made a calculation mistake when they were trying to justify their assumptions on the role of the negative curvature of the core boundary. The mistake was made when calculating the waveguide loss for a dielectric tube using an analytical formula from [Marcatili & Schmeltzer, 1964]. Indeed, the loss levels for the dielectric tube and silica HC MF with the cladding consisting of solid rods with equal air core diameters are approximately the same. Despite this fact, the main conclusion of the paper remains accurate, i.e. that to obtain a long wavelength waveguide regime in the mid IR with silica HC MF it is necessary to combine two factors, namely, the negative curvature of the core boundary and the low density of eigenstates of the individual elements of the cladding.

To clarify a role of the negative curvature of the core boundary we should consider a plane wave scattering on the curved surface, for example, of a solid rod. This problem was solved by many authors [Wait, 1955; Lind & Greenberg, 1966]. Depending on the polarization state of the incident plane wave z - component of the electric (TM polarization) or magnetic field (TE polarization) is parallel to the incident plane. Suppose the refractive index of the solid rod is n_1 and the outer space is n_2 . In the following, only TE polarized plane wave will be considered. Its z - component of the magnetic field can be expanded according to addition theorem for Bessel functions and taking into account the temporal dependence as $e^{i\omega t}$ one can obtain:

$$H_z^i = H_0 \sin \theta \left[\sum_{n=-\infty}^{\infty} i^n J_n(\lambda_2 r) e^{-in\varphi} \right] e^{-i\beta z}$$

$$E_z^i = 0, \quad (1)$$

where θ is an angle of incidence, φ and r are an azimuthal and radial cylindrical coordinates, H_0 is an amplitude of the incident plane wave and $J_n(\lambda_2 r)$ are the Bessel functions of first kind. If $k_2 = \frac{2\pi}{\lambda} n_2$ is a wavevector in the outer space $\lambda_2 = \sqrt{k_2^2 - \beta^2}$ is its transverse component and $\beta = k_2 \cos \theta$ is its axial component. In such a way, the incident

plane wave is expanded into an infinite number of cylindrical harmonics due to the curvature of the cylinder surface. The z - components of the scattered field and field inside the cylinder can be expressed in the same manner:

$$H_z^s = \left[\sum_{n=-\infty}^{\infty} b_n^s H_n^{(2)}(\lambda_2 r) e^{-in\varphi} \right] e^{-i\beta z}$$

$$E_z^s = \left[\sum_{n=-\infty}^{\infty} a_n^s H_n^{(2)}(\lambda_2 r) e^{-in\varphi} \right] e^{-i\beta z} \quad (2a)$$

$$H_z^{ins} = \left[\sum_{n=-\infty}^{\infty} b_n J_n(\lambda_1 r) e^{-in\varphi} \right] e^{-i\beta z}$$

$$E_z^{ins} = \left[\sum_{n=-\infty}^{\infty} a_n J_n(\lambda_1 r) e^{-in\varphi} \right] e^{-i\beta z}, \quad (2b)$$

where $H_n^{(2)}(\lambda_2 r)$ is Hankel function, $\lambda_1 = \sqrt{k_1^2 - \beta^2}$ is a transverse components of the wavevector $k_1 = \frac{2\pi}{\lambda} n_1$ for the field inside the rod. On the basis of these expressions for z - components of the incident, scattered and inside fields it is possible to calculate φ and r - components of the fields [Adler, 1952]. In other words, the field of the incident wave is represented by an infinite number of space 'channels' (harmonics) through which the energy of the incident wave is transferred to the scattered fields and the fields inside the dielectric rod. It is seen, that such sets of cylindrical harmonics (1) - (2) have a mode structure and can be considered as radiation or continuous modes of ITE (incident transverse electric) type of the individual dielectric rod [Snyder, 1971].

To calculate the coefficients b_n^s, a_n^s, b_n, a_n it is necessary to apply boundary conditions for z and φ - components of the incident, scattered fields and the fields inside the cylinder. Because of the mode structure of the total field it is not necessary to solve an infinite set of simultaneous linear equations. To obtain the n th order coefficients one needs to solve 4*4 inhomogeneous system of linear equations. For a solid cylinder rod it is possible to obtain analytical expression for the coefficients which includes such terms as $J_n'(\lambda_1 a) / J_n(\lambda_1 a)$ [Wait, 1955]. These terms have resonances (poles) corresponding to zeros of $J_n(\lambda_1 a)$. It is necessary to point out that the resonances of the n th order coefficients of the scattered field are determined not only by n th order functions $J_n(\lambda_1 a)$ but also by $J_{n+1}(\lambda_1 a)$ and $J_{n-1}(\lambda_1 a)$ due to recurrent relations for the derivatives of the Bessel functions. In other words, the different diffraction orders are coupled between each other. Due to this fact, it is possible to observe not only Lorentzian - like resonances for the spectral dependencies of absolute values of the amplitudes $|b_n^s|, |a_n^s|$ but also Fano type resonances [Fano, 1961]. For example, Fano type resonances were analysed in the case of all solid band gap fibers [Steinvurzel et. al., 2006] with the cladding consisting of solid dielectric cylinders with a refractive index higher than the background.

A similar phenomenon occurs when the plane wave is scattered on optical diffraction grating. A short analysis can be carried out based on the work [Hessel & Oliner, 1965].

Suppose the diffraction grating extends infinitely in the y and z directions, with the period d in the z direction only. The refractive index of the outer medium is again n_2 . The magnetic field of this incident wave of S polarization is represented as:

$$H_y^i = H_0 e^{ik_x x} e^{-i\beta z} \quad (3)$$

Then, due to periodicity the scattered magnetic field can be represented as [Hessel & Oliner, 1965]:

$$H_y^s = \left[\sum_{n=-\infty}^{\infty} A_n(\beta) e^{ik_x^n x} e^{-i\frac{2\pi n}{d} z} \right] e^{-i\beta z}, \quad (4)$$

where $A_n(\beta)$ are the amplitudes of the various spectral orders and $k_x^n = \sqrt{k_2^2 - (\beta + \frac{2\pi n}{d})^2}$ are transverse components of the wavevector of the scattered field. Applying boundary conditions one obtains an infinite inhomogeneous set of simultaneous linear equations [Hessel & Oliner, 1965] for the scattered field amplitudes $A_n(\beta)$. These amplitudes are coupled between each other as in the case of the plane wave scattering on the rod and a set of resonances Lorentzian and Fano types known as Wood anomalies [Wood, 1902; Lord Rayleigh, 1907; Hessel & Oliner, 1965] also occur. In the case of optical grating the conservation of light momentum for the scattered light in the z - direction looks like:

$$k_n^s = \beta + \frac{2\pi n}{d}.$$

In the case of the plane wave scattering on a dielectric rod there is also a conservation of the angular momentum of the light. The fields of the source plane wave are expanded into a set of the 'space' channels with an angular momentum determined by the number of n in $e^{-in\phi}$ (1) and each continuous (radiation) mode of the dielectric rod has the same angular momentum (1, 2). Note, that this is (4) of the same form as an expression (2a) for the scattered field H_z^s in the case of the dielectric rod. Comparing expressions (2a) and (4) one can state that the process of the plane wave scattering on the rod can be represented as scattering on the diffraction quasi - grating. The surface of the dielectric rod can be considered as an azimuthal diffraction grating with periodicity in ϕ - direction and conservation of the angular momentum of the light. But instead of one incident plane wave as in the case of the plane diffraction grating (3) there is an infinite set of incident cylindrical harmonics with their own angular momentums of the light. It can also be shown that the spectral dependencies of b_n^s, a_n^s in expansions (2a) demonstrate the resonance behaviour analogous to Wood anomalies as in the case of the plane diffraction grating. This problem and its application to the waveguide mechanism in all solid band gap fibers will be considered by us thoroughly in our future publication. In the same way, it is possible to consider a cylindrical surface of the capillary as a diffraction quasi - grating in the ϕ direction instead of z - direction in the case of the plane diffraction grating.

The main conclusion to draw is that the plane wave incidence on a curved cylindrical surface leads to the appearance of an infinite set of cylindrical harmonics with different

angular momentums of the light. As the source of the incident wave is outside of a solid cylinder or a capillary one obtains an inhomogeneous set of linear equations for determining amplitudes of the scattered field harmonics. These scattered field harmonics have the same values of the angular momentums of the light as the harmonics of the incident field. Different orders of these harmonics (diffraction orders) are coupled between each other due to the properties of the Bessel functions. It leads to appearance of Wood anomalies in the spectral dependencies of their amplitudes. As a consequence, the curved cylindrical surface can be considered as an azimuthal diffraction grating with modulation in φ - direction [Pryamikov, to be prepared]. This fact leads to a loss of simplicity of the boundary conditions for the air core modes of the HC MF with the cladding consisting of capillaries compared with BG HC PCF, for example. Similar situation occurs if one considers the boundary conditions for the core modes of all solid photonic band gap fibers [White et. al., 2002] and Bragg fibers [Yeh et. al., 1978].

3.2 Discrete rotational symmetry of the core boundary

Another aspect of the problem of complicated boundary conditions for HC MF with the cladding consisting of N capillaries is that the capillary location in the cladding is also periodic in the azimuthal coordinate φ (Fig.1). As a result, the boundary conditions for the air core modes are also periodic. It is known that if the system transforms into itself for a set of discrete rotations $\delta\varphi = 2\pi k / N$, $k \in (0, N - 1)$ around axial vector \vec{z} the eigenfunctions of the system (in other words, the air core modes) can be represented as [Skorobogatiy & Yang, 2009]:

$$\psi_n(r, \varphi, z) = e^{-in\varphi} U_n(r) e^{-i\beta z}, \quad (5)$$

and their eigenvalues are:

$$X = e^{in \frac{2\pi k}{N}}.$$

These eigenvalues are the same for any $n = n + Nm$, where m is an integer and the eigenfunctions characterized by an integer n are degenerate ones [Skorobogatiy & Yang, 2009]. As a consequence, such eigenstates of the system with a discrete rotational symmetry can be expressed as a superposition of all the degenerate states:

$$\psi_n(r, \varphi, z) = \left[\sum_{m=-\infty}^{\infty} A(m) U_{n+Nm}(r) e^{-i(n+Nm)\varphi} \right] e^{-i\beta z}, \quad (6)$$

where an expression under the sum sign is a periodic function in φ with a period $\frac{2\pi}{N}$ and $n \in [0, N - 1]$. Note that this is (6) of the same form as an expression (2a) and (4) for the scattered field H_z^s in the case of the dielectric rod and the plane diffraction grating. The discrete symmetry of the core boundary gives one more type of azimuthal diffraction grating in the considered HC MFs.

In such a way, the boundary conditions for the air core modes of the HC MF with the cladding consisting of capillaries are complicated not only by the curvature of the

cylindrical surface of an individual capillary but also by the discrete rotational symmetry of the core boundary.

3.3 Complicated boundary conditions for the air core mode of HC MF with the cladding consisting of capillaries and low loss guidance

Summarizing the conclusions of the two previous subsections one can state that the air core modes of HC MFs with the cladding consisting of capillaries are formed by a superposition (interference) of several space cylindrical harmonics originated from the azimuthal diffraction quasi - gratings occurred in the cladding. The main factors affecting the air core mode formation are geometry parameters of an individual capillary and the type of a periodic arrangement of the capillaries in the cladding. All these space harmonics interact with the capillary walls in stronger or weaker ways depending on their radial and azimuthal distribution. In this case, the material loss of the capillary walls doesn't have the same affect on the attenuation of each harmonic. In such a way, the energy of the air core mode at the core boundary for HC MF with the cladding consisting of capillaries is distributed in much more complicated way than in the case of BG HC PCFs or kagome lattice IC HC PCFs.

BG HC PCFs and kagome lattice IC HC PCFs do not have such complicated mechanism of the air core modes formation because of a quasi continuous rotational symmetry of the core boundary and the boundaries of succeeding layers in the cladding. Kagome lattices IC HC PCFs sometimes have the discrete symmetry of the core boundary but just with a polygonal shape of the core without a negative curvature of the core boundary. The authors in [Pearce et al., 2007] have shown that the loss behavior of a hollow core fiber with the cladding consisting of concentric glass rings or hexagons explain the qualitative features in the loss curves associated with kagome lattice IC HC PCF. The hollow core photonic band gap fiber with the cladding consisting of concentric glass rings has a continuous rotational symmetry of the core modes and is analogous to solid Bragg fibers [Fevrier et. al., 2006]. In this case, the air core is formed by the boundaries of the concentric glass rings which cannot play the role of the azimuthal diffraction gratings. Applying boundary conditions to each concentric ring of the cladding one obtains a homogeneous system of linear equations determinant of which is a dispersion relation for the air core modes. Each air core mode is formed and described by only one space cylindrical harmonic with the propagation constant β determined from the corresponding dispersion relation. These space harmonics don't interact with each other's as in the case of all solid band gap fibers and Fano type resonances cannot be observed (an exception can be kagome lattice IC HC PCF with a polygonal shape of the air core). As a consequence, all energy of each air core mode is concentrated in one 'space' channel (cylindrical harmonic) which interacts with glass rings of the cladding in the same way according to its azimuthal angular dependence of $e^{-im\varphi}$. This air core mode is leaky and its imaginary part of β is determined from the dispersion relation mentioned above. All resonances in high index layers for this mode are radial and can be described by the ARROW model [Litchinitser et. al., 2002].

The other very important moment is that the geometry parameters of the capillaries d_{ins}, d_{out} and the glass refractive index at the determined value of D_{core} (Fig .1(left)) should be chosen

in such a way so as to excite leaky modes with high quality factor. These modes usually have high radial and azimuthal indices. To this end, the capillary wall thickness must be thin enough and comparable with the wavelength. In this case, it is possible to obtain large widths of the transmission regions for the air core modes. Moreover, it seems possible to choose all parameters of the considered HC MF including glass refractive index in such a way so as to obtain a very weak interaction (coupling) of each cylindrical harmonic constituting the air core mode with capillary walls inside the transmission regions. All these factors can give rise to a low loss waveguide regime for CO₂ laser radiation. Several examples of such waveguide regimes will be given in the next section.

4. Numerical modelling of HC MFs with different types of discrete rotational symmetry of the core boundary and glass composition of the capillaries

In the following subsections four types of HC MFs with the claddings consisting of 6, 8, 10 and 12 capillaries will be considered. The calculations will be carried out for two values of the glass refractive indices $n = 2.4, 2.8$ and with three values of $d_{ins} / d_{out} = 0.8, 0.85, 0.9$. All calculations will be made in the narrow spectral region near $\lambda = 10.6 \mu\text{m}$. This fact is connected with high density of the individual capillary eigenstates (leaky modes with high azimuthal indices [Vincetti & Setti, 2010]) which occur at such high values of the glass refractive indices and individual capillary dimensions with respect to the wavelength. We will show that the way of obtaining a low loss waveguide regime in the glass HC MFs with the cladding consisting of capillaries presents a complicated multiparameter task. Unusual behaviour of the bend loss depending on the bend radii for high index glass HC MFs with the cladding consisting of capillaries will be demonstrated.

4.1 Loss dependencies for HC MF with different number of capillaries in the cladding

First, we will consider the loss dependencies for HC MF with six capillaries in the cladding. As was mentioned above, all loss dependencies are calculated in the narrow spectral range from $10.59 \mu\text{m}$ to $10.61 \mu\text{m}$ with a wavelength step equals to 1 nm. The calculations will be made for two values of the ratio of $d_{ins} / d_{out} = 0.85$ and 0.9 because the losses are very high at lower values of the one. In Fig. 2 these dependencies are shown for two values of the air core diameter $D_{core} = 220 \mu\text{m}$ and $320 \mu\text{m}$.

As one can see from Fig. 2(a) HC MF with $n = 2.4$ and $d_{ins} / d_{out} = 0.9$ has the minimal loss level in the considered spectral range. In our opinion, it can be explained by the minimal value of density of individual capillary states. In this case, the capillary has a minimal capillary wall thickness with respect to the wavelength and the lowest refractive index. The loss dependence for HC MF with $n = 2.8$ and $d_{ins} / d_{out} = 0.9$ is relatively inhomogeneous and has a strong peak at $\lambda = 10.601 \mu\text{m}$ caused by the excitation of a capillary leaky mode with high azimuthal and radial indices. This mode is shown in Fig. 3(left).

Other curves in Fig.2 (a) for $d_{ins} / d_{out} = 0.85$ have a higher loss level due to thicker capillary walls compared to the previous case. In Fig. 2(b) HC MF with $n = 2.8$ and $d_{ins} / d_{out} = 0.85$ has the maximal loss due to the excitation of the second type of the capillary leaky modes.

These capillary modes have a lower azimuthal index and a different radial dependence (Fig. 3(right)). It is worth pointing out that these two types of the individual capillary leaky modes are the main reason for occurring high loss regions for the considered HC MFs made of high index glasses.

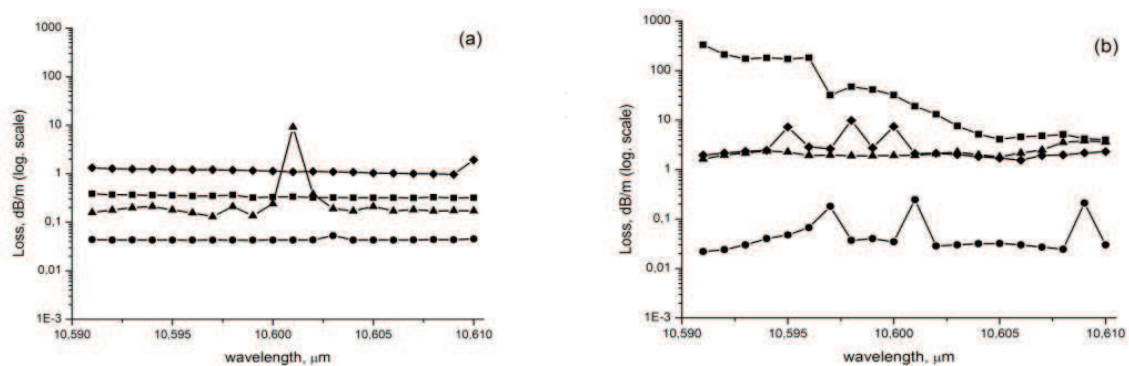


Fig. 2. (a) loss dependence for HC MF with $D_{core} = 220 \mu\text{m}$ and 6 capillaries in the cladding, $d_{ins} / d_{out} = 0.9$ ($n = 2.4$, circles), $d_{ins} / d_{out} = 0.9$ ($n = 2.8$, triangles), $d_{ins} / d_{out} = 0.85$ ($n = 2.4$, rhombuses), $d_{ins} / d_{out} = 0.85$ ($n = 2.8$, squares); (b) loss dependence for HC MF with $D_{core} = 320 \mu\text{m}$ the other notations are the same as in (a).

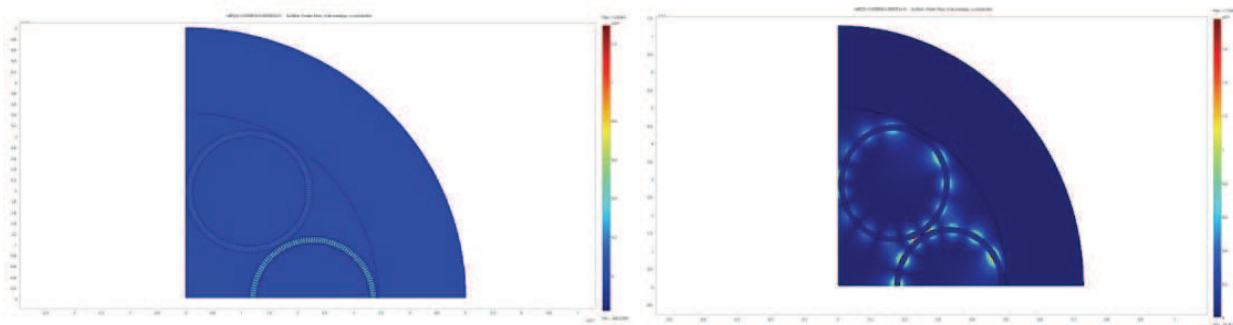


Fig. 3. (left) a typical Pointing vector distribution for a capillary leaky mode in the cladding with a high azimuthal index; (right) the Pointing vector distribution for the second type of the capillary leaky modes with a lower azimuthal index.

Further, we will consider HC MF with eight capillaries in the cladding. The air core diameters and the glass refractive indices will be the same as in the case of HC MFs with six capillaries in the cladding. In Fig. 4 the loss dependencies for this HC MF are shown.

As one can see from Fig. 4(a) HC MF with $d_{ins} / d_{out} = 0.85$ and $n = 2.8$ has the highest loss due to the excitation of the leaky modes with a lower azimuthal index in this spectral region (Fig. 3(b)). The HC MF with $d_{ins} / d_{out} = 0.85$ and $n = 2.4$ has a high loss for the same reason. Losses for HC MFs with other parameters in Fig. 4(a) are relatively low, especially, in the case of HC MF with $d_{ins} / d_{out} = 0.8$ and $n = 2.4$. The losses for HC MFs with $D_{core} = 320 \mu\text{m}$ are very high due to the strong coupling of the air core modes with the capillary modes having a lower azimuthal index (Fig.3(right)) in this spectral range with the exception of the HC MF with $d_{ins} / d_{out} = 0.85$ and $n = 2.8$.

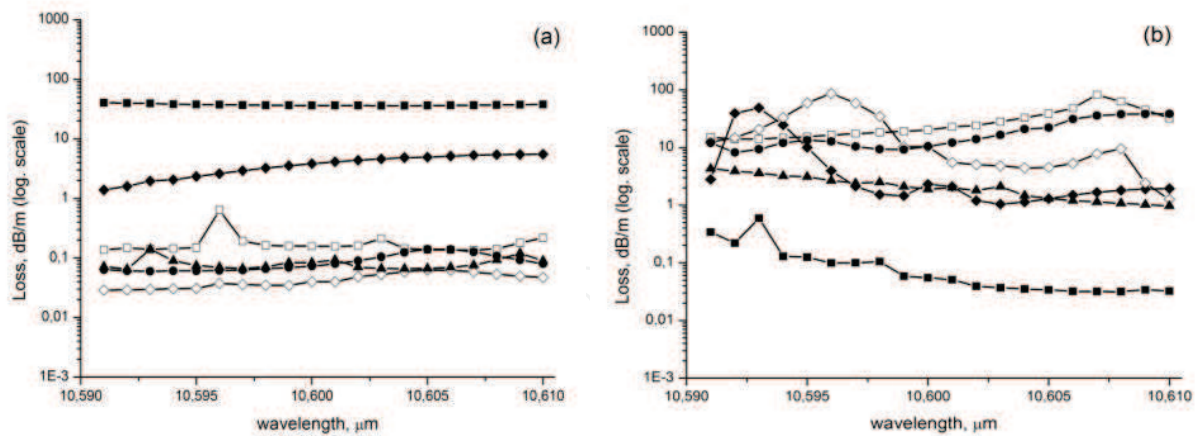


Fig. 4. (a) loss dependence for HC MF with $D_{core} = 220 \mu\text{m}$ and 8 capillaries in the cladding, $d_{ins} / d_{out} = 0.9$ ($n = 2.4$, circles), $d_{ins} / d_{out} = 0.9$ ($n = 2.8$, triangles), $d_{ins} / d_{out} = 0.85$ ($n = 2.4$, rhombuses), $d_{ins} / d_{out} = 0.85$ ($n = 2.8$, squares), $d_{ins} / d_{out} = 0.8$ ($n = 2.4$, white rhombuses), $d_{ins} / d_{out} = 0.8$ ($n = 2.8$, white squares); (b) loss dependence for HC MF with $D_{core} = 320 \mu\text{m}$ the other notations are the same as in (a).

The loss dependencies for HC MFs with ten capillaries in the cladding are shown in Fig. 5. The values of d_{ins} , d_{out} and consequently the capillary wall thicknesses are lower compared to the cases considered above. The loss level for all HC MFs (Fig. 5(a)) is very high due to a strong coupling to the individual capillary leaky modes of both types. Low loss curves correspond only to HC MFs with $d_{ins} / d_{out} = 0.8$, 0.85 and $n = 2.8$. The other picture is observed in the case of HC MFs with $D_{core} = 320 \mu\text{m}$. All loss dependencies have low losses with the exception of HC MF with $d_{ins} / d_{out} = 0.8$ and $n = 2.8$ which has strong coupling with the cladding and, consequently, a non propagating regime in this spectral range.

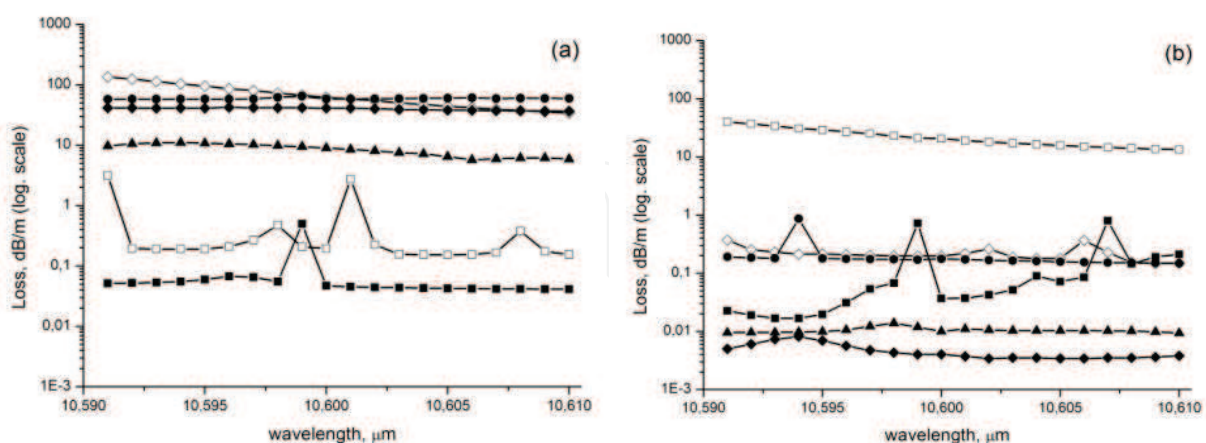


Fig. 5. (a) loss dependence for HC MF with $D_{core} = 220 \mu\text{m}$ and 10 capillaries in the cladding, $d_{ins} / d_{out} = 0.9$ ($n = 2.4$, circles), $d_{ins} / d_{out} = 0.9$ ($n = 2.8$, triangles), $d_{ins} / d_{out} = 0.85$ ($n = 2.4$, rhombuses), $d_{ins} / d_{out} = 0.85$ ($n = 2.8$, squares), $d_{ins} / d_{out} = 0.8$ ($n = 2.4$, white rhombuses), $d_{ins} / d_{out} = 0.8$ ($n = 2.8$, white squares); (b) loss dependence for HC MF with $D_{core} = 320 \mu\text{m}$ the other notations are the same as in (a).

The loss dependencies in Fig. 5 show that a low loss regime for the high index glass HC MFs with the cladding consisting of capillaries can be obtained by the right selection of many parameters characterizing HC MF including D_{core} .

At the end of this subsection, the loss dependencies for HC MFs with the cladding consisting of 12 capillaries will be shown (Fig. 6).

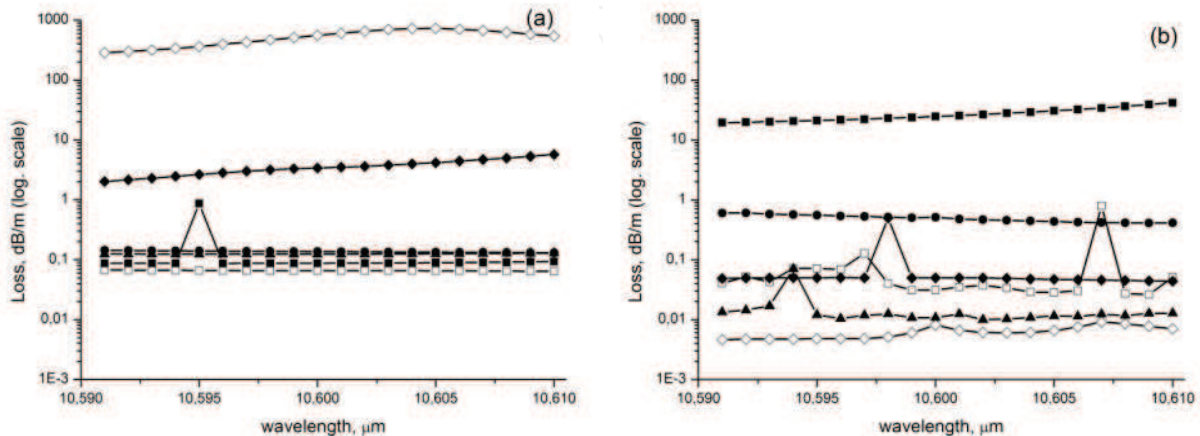


Fig. 6. (a) loss dependence for HC MF with $D_{core} = 220 \mu\text{m}$ and 12 capillaries in the cladding, $d_{ins} / d_{out} = 0.9$ ($n = 2.4$, circles), $d_{ins} / d_{out} = 0.9$ ($n = 2.8$, triangles), $d_{ins} / d_{out} = 0.85$ ($n = 2.4$, rhombuses), $d_{ins} / d_{out} = 0.85$ ($n = 2.8$, squares), $d_{ins} / d_{out} = 0.8$ ($n = 2.4$, white rhombuses), $d_{ins} / d_{out} = 0.8$ ($n = 2.8$, white squares); (b) loss dependence for HC MF with $D_{core} = 320 \mu\text{m}$ the other notations are the same as in (a).

It has thus been shown that the achievement of a low loss waveguide regime for HC MFs with the cladding consisting of capillaries is complicated multi parameter task. All the parameters characterizing the HC MFs such as D_{core} , d_{ins} , d_{out} , n , N (number of the capillaries in the cladding) have an effect on the waveguide regime in the considered spectral range. In this way, two main factors affect the loss level of the HC MFs. The first is the density of eigenstates of the individual capillary and the second is the discrete rotational symmetry of the core boundary. The density of eigenstates of the individual capillary is determined by geometry parameters of a capillary and the value of a glass refractive index. The second factor is connected to the symmetry of the capillary arrangement in the cladding. By comparing the figures in this subsection one can make a conclusion that by decreasing the number of capillaries in the cladding one obtains a stronger dependence on the D_{core} . It seems possible to find a balance between the number of capillaries and the air core diameter. With the increase in the capillary number the role of the discrete rotational symmetry weakens.

4.2 Bend loss dependencies on a bend radius for HC MF with a different number of capillaries in the cladding

In this subsection we will consider characteristics of the bend loss behaviour for HC MFs with a different number of capillaries in the cladding. To reveal the special features of the bend loss one analyses the bend loss behaviour for HC MFs with optimal waveguide

regimes found in the previous subsection and, correspondingly, with minimal waveguide losses.

In Fig.7 the bend loss dependencies for two low loss waveguide regimes in the case of HC MF with the cladding consisting of 6 capillaries and 8 capillaries are shown.

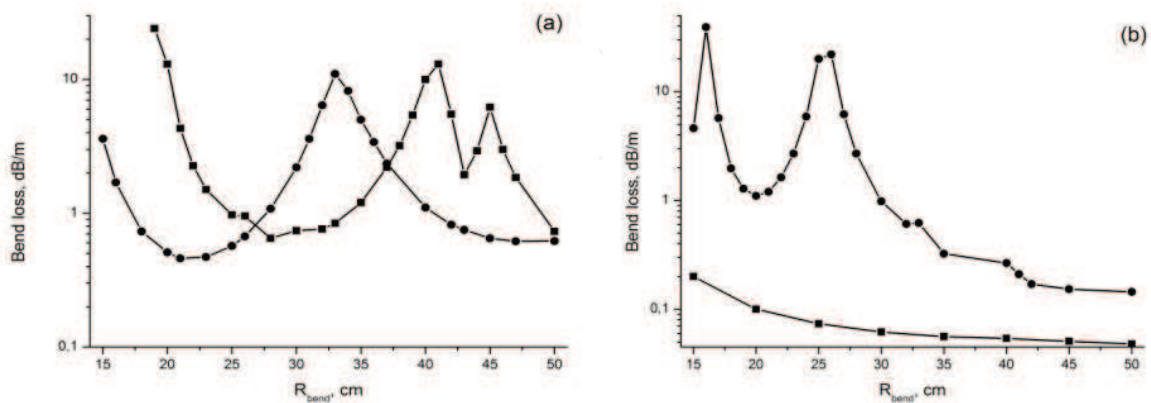


Fig. 7. (a) bend loss dependence on the bend radius for HC MFs with 6 capillaries in the cladding: $D_{core} = 220 \mu\text{m}$, $d_{ins}/d_{out} = 0.9$ ($n = 2.4$, squares) and $D_{core} = 320 \mu\text{m}$, $d_{ins}/d_{out} = 0.9$ ($n = 2.4$, circles); (b) bend loss dependence on the bend radius for HC MFs with 8 capillaries in the cladding: $D_{core} = 220 \mu\text{m}$, $d_{ins}/d_{out} = 0.8$ ($n = 2.4$, squares) and $D_{core} = 320 \mu\text{m}$, $d_{ins}/d_{out} = 0.85$ ($n = 2.8$, circles).

As one can see from Fig. 7(a), the bend loss dependencies have resonance peaks in the case of both values of D_{core} . Just as in the case of HC MF with 8 capillaries in the cladding this resonance behaviour exists only for HC MF with $D_{core} = 320 \mu\text{m}$ (Fig. 7(b)). These resonances are connected with the excitation of capillary eigenstates modes called 'airy' modes [Vincetti&Setti, 2010]. An example of such a resonance tunnelling with the excitation of the 'airy' mode of the individual capillary under bending is shown in Fig. 8 for HC MF with 8 capillaries in the cladding.

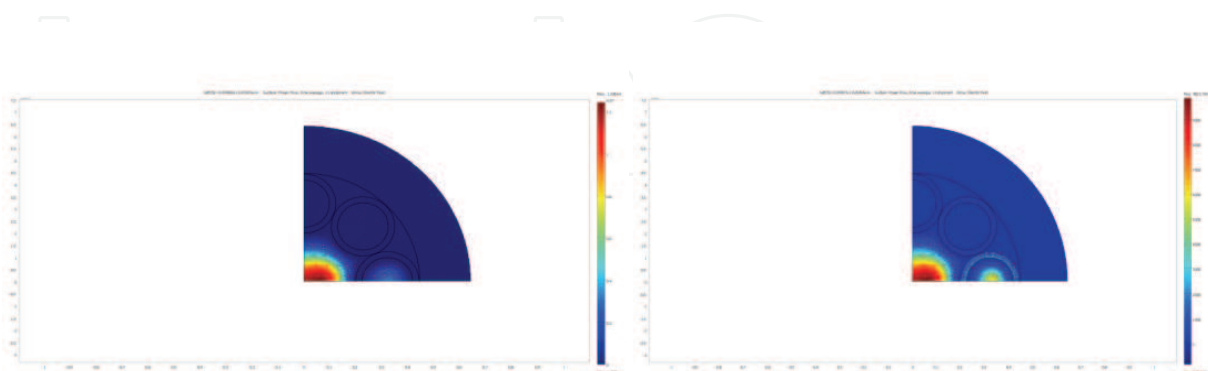


Fig. 8. (left) the air core mode of HC MF with 8 capillaries in the cladding begin to couple with an 'airy' mode of an individual capillary of the cladding at a certain value of the bend radius; (right) the resonance excitation of the 'airy' mode of an individual capillary occurs at a lower value of the bend radius.

Such resonance behaviour of the bend loss occurs due to a very high density of dielectric modes (eigenstates) of an individual capillary at such values of n , d_{ins} , d_{out} . The energy of the air core mode of the HC MFs is tunnelled by these dielectric modes into the capillary 'airy' modes. The higher the values of n , d_{ins} , d_{out} with respect to the wavelength the more effective tunnelling is observed and the excited 'airy' modes of the individual capillary have higher quality factor. For example, the bend loss dependence for HC MF with the cladding consisting of 8 capillaries and $D_{core} = 220 \mu\text{m}$ has no resonance peaks due to suppressing the tunnelling through the capillary walls due to a decrease in the values of d_{ins} , d_{out} or n .

To confirm the above conclusions, bend losses for HC MFs with the cladding consisting of 10 and 12 capillaries were calculated (Fig. 9). As in the case of Fig. 7, HC MFs with the lowest waveguide losses were taken for the bend loss calculations.

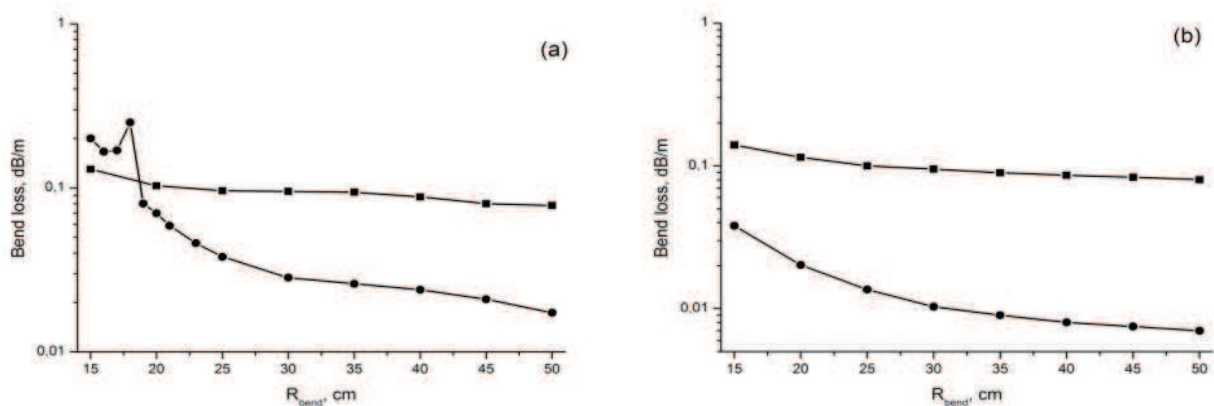


Fig. 9. (a) bend loss dependence on the bend radius for HC MFs with 10 capillaries in the cladding: $D_{core} = 220 \mu\text{m}$, $d_{ins} / d_{out} = 0.85$ ($n = 2.8$, squares) and $D_{core} = 320 \mu\text{m}$, $d_{ins} / d_{out} = 0.85$ ($n = 2.4$, circles); (b) bend loss dependence on the bend radius for HC MFs with 12 capillaries in the cladding: $D_{core} = 220 \mu\text{m}$, $d_{ins} / d_{out} = 0.8$ ($n = 2.8$, squares) and $D_{core} = 320 \mu\text{m}$, $d_{ins} / d_{out} = 0.8$ ($n = 2.4$, circles).

All curves in Fig. 9 have no resonance peaks except for the HC MF with $D_{core} = 320 \mu\text{m}$, $d_{ins} / d_{out} = 0.85$ and $n = 2.4$. In this case, the dielectric capillary mode with a high azimuthal index (Fig. 3(left)) was excited at the bend radius $R = 18 \text{ cm}$ and a weak tunnelling process into the 'airy' mode occurred. The level of the bend losses for all considered bent HC MFs (Fig. 9) is very close to that of the straight HC MFs.

In conclusion, one can state that the optimal waveguide regime in the spectral region near $\lambda = 10.6 \mu\text{m}$ for HC MFs made of high index glass ($n > 2$) is possible at $N > 8$, where N is a number of capillaries in the cladding. In this case, the process of tunnelling of the air core modes of HC MF into the 'airy' modes of an individual capillary is suppressed due to low quality factor of the 'airy' modes and thus a low loss waveguide regime for a bend becomes possible.

5. Conclusion

The guidance of CO₂ laser radiation in HC MFs with the cladding consisting of capillaries was analysed. Two main factors affecting the waveguide mechanism in these waveguide

structures were proposed. The first factor is connected with the representation of the curved air core boundary of the HC MFs as azimuthal diffraction quasi - gratings. These azimuthal diffraction gratings occur due to the cylindrical surface of an individual capillary of the cladding as well as to a discrete rotational symmetry of their arrangement in the cladding. In this way, the air core mode of the HC MF is formed by the interference of space cylindrical harmonics originated from the light scattering on these quasi - diffraction gratings. The process of the air core mode formation is much more complicated compared to the one for the HC MFs with continuous rotational symmetry of the air core boundary. The interaction of cylindrical harmonics forming the air core mode of the HC MF with the capillary walls is different from each other. It leads to a weakened material loss effect on the waveguide regime in comparison with the HC MF with a continuous rotational symmetry of the air core boundary, for example, IC HC PCFs. The second factor is connected with the optical properties of an individual capillary, in particular, with the density of its eigenstates (leaky modes). This factor determines the widths of the transmission regions and the level of waveguide losses. Numerical analyses have shown that a low loss waveguide regime in the spectral region near $\lambda = 10.6 \mu\text{m}$ for the HC MFs with the cladding consisting of high index glass capillaries becomes possible. The optimisation of the HC MF structure to achieve these regimes is a complicated multiparameter task depending on all geometry parameters characterizing the HC MFs and the value of a glass refractive index. The bend loss of the HC MFs with the cladding consisting of capillaries made of high index glasses has a resonance character depending on the bend radius. To suppress such resonances it is necessary to increase the number of capillaries in the cladding. It leads to a decrease in the capillary sizes and to a decrease in the quality factor of the 'airy' modes of the capillaries.

In the end, we would like to outline the prospects of future investigations in this field. In our opinion, to improve the waveguide properties of the HC MFs it is necessary to study the process of the air core mode formation more carefully. An effect of different types of symmetries of the capillaries arrangements in the cladding and the value of D_{core} on the level of waveguide loss should be investigated. The optical properties of an individual capillary made of high index glass, in particular, its optical eigenstates and the density of these eigenstates depending on the geometry parameters of the capillary and glass refractive indices should be studied. To achieve a low loss guidance it is necessary to perform an optimisation of the HC MFs structure. This complicated optimisation task can be performed by powerful numerical algorithms which have already been applied, for example, to optimisation of the Bragg fibers structures [Biriukov et. al., 2008]. Also, it is necessary to improve the technology of making high index glasses with a low material loss and a technology of the HC MFs fabrication. It is worth mentioning that the early experiments demonstrated the possibility of obtaining waveguide regimes for such HC MFs made of high index chalcogenide glasses at CO₂ laser wavelengths [Kosolapov et. al., 2011]. As the light was well localized in the core, such fibers hold much promise for the delivery of CO₂ laser radiation.

6. Acknowledgment

The authors thank Alexandra Nikolskaya for her assistance in translating this chapter into English.

7. References

- Abel, T., Hirsch, J., Harrington, J. (1994). Hollow glass waveguides for broadband infrared transmission. *Optics Letters*, Vol.19, No.14, pp. 1034-1036.
- Adler R. B. (1952). Proceedings Of the I. R. E., Vol. 40, p. 339 - 348.
- Benabid F., Knight J. C., Antonopoulos G., Russell P. St. J. (2002). Stimulated Raman scattering in hydrogen - filled hollow core photonic crystal fibers. *Science*, Vol. 298, pp. 399 - 402.
- Benabid, F., Bowmans, G., Knight, J.C., Russell, P.St.J., Couny, F. (2004). Ultrahigh efficiency laser wavelength conversion in a gas - filled hollow core photonic crystal fiber by pure stimulated rotational Raman scattering in molecular hydrogen. *Physical Review Letters*, Vol.93, No.12, pp. 123903-4.
- Biriukov A. S.; Bogdanovich D. V.; Gaponov D. A.; Pryamikov A. D. (2008). Optical properties of Bragg fibers. *Quantum Electronics*, Vol.38, pp. 620 - 633.
- Birks T. A., Roberts P. J., Russell P.S., Atkin D. M., and Shepherd T. J. (1995). Full 2- D photonic band gaps in silica/air structures. *Electron. Letters*, Vol. 31, p. 1941 - 1943.
- Bowden B. F.&Harrington J. A. (2009). Fabrication and characterization of chalcogenide glass for hollow Bragg fibers. *Applied Optics*, Vol.48, pp. 3050 - 3054.
- Croitoru N., Saba K., Dror J., Goldenberg E., Mendelovic D., and Israel G. (1990). U.S. Patent 4.390.863.
- Croitoru N., Dror J., and Gannot I. (1990). Characterization of hollow fibers for the transmission of infrared radiation. *Appl. Optics*, Vol. 29, p. 1805 - 1809.
- Deseveday F.; Renversez G.; Troles J.; Houzot P.; Brilland L.; Vasilief I.; Coulombier Q.; Traynor N.; Smektala F.; Adam J -L. (2010). Chalcogenide glass hollow core photonic crystal fibers. *Optical Materials*, Vol.32, pp. 1532 - 1539.
- Fano U. (1961). Effects of configuration interaction on intensities and phase shifts. *Phys. Review*, Vol.124, pp. 1866 - 1878.
- Fevrier S.; Jamier R.; Blondy J -M.; Semjonov S. L.; Likhachev M. E.; Bubnov M. M.; Dianov E. M.; Khopin V. F., Salganskii M. Y., Guryanov A. N. (2006). Low loss singlemode large mode area all silica photonic band gap fiber. *Optics Express*, Vol.14, pp. 562 - 569.
- Garmire, E., McMahon, T., Bass, M. (1976). Propagation of infrared light in flexible hollow waveguides. *Applied Optics*, Vol.15, No.1, pp.145 -150.
- Garmire, E., McMahon, T., Bass, M. (1979). Low-loss propagation and polarization rotation in twisted infrared metal waveguides. *Appl. Phys. Letters*, Vol.34, No.1, pp. 35-37.
- Gregan R. F., Mangan B. J., Knight J. C., Birks T.A., Russell P. St. J., Roberts P. J., and Allan D.C. (1999). Single - mode photonic band gap guidance of light in air. *Science*, v. 285, pp. 1537 - 1539.
- Harrington J.A., Gregory, C.C. (1990). Hollow sapphire fibers for the delivery of CO₂ laser energy. *Optics Letters*, Vol.15, No.10, pp.541-543.
- Hessel A.&Oliner A. A. (1965). A new theory of Wood's anomalies on optical gratings. *Applied Optics*, Vol.4, pp. 1275 - 1297.
- Hongo, A., Morosawa, K., Matsumoto, K., Shiota, T., Hashimoto, T. (1992). Transmission of kilowatt - class CO₂ laser light through dielectric - coated metallic hollow waveguides for material processing. *Applied Optics*, Vol.31, No.24, pp. 5114-5120.

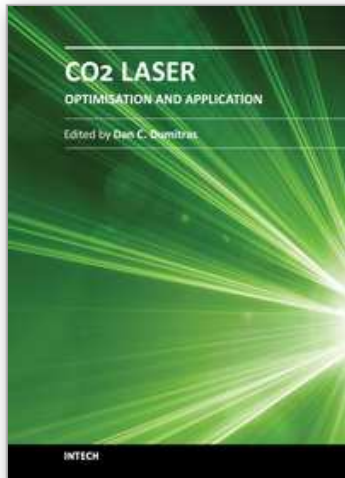
- Hu J. & Menyuk C. R. (2007). Leakage loss and bandgap analysis in air – core photonic bandgap fiber for nonsilica glasses. *Optics Express*, Vol.15, pp. 339 - 349.
- Humbert G., Knight J. C., Bowmans G., Russell P. St. J., Williams D. P., Roberts P. J., and Mangan B. J. (2004), Hollow core photonic crystal fibers for beam delivery. *Opt. Express*, Vol. 12, pp. 1477 - 1484.
- Karasawa S., Miyagi M., Nakamura T., Ishikawa H. (1990). Fabrication of dielectric – coated waveguides for CO₂ laser light transmission. *Electronics and Communications in Japan (Part 2: Electronics)*, Vol. 73, Issue 6, pp. 65 - 69.
- Kosolapov A.; Pryamikov A.; Biriukov A.; Astapovich M.; Shiryaev V.; Snopatin G.; Plotnichenko V.; Churbanov M.; Dianov E. (2011). Demonstration of CO₂ – laser power delivery through chalcogenide – glass fiber with negative – curvature hollow core. *Optics Express*, Vol. 19, pp. 25723 - 25728.
- Laakmann K. (1987). U.S. Patent 4.688.893.
- Lind A. C. & Greenberg J. M. (1966). Electromagnetic scattering by obliquely oriented cylinders. *Journal of applied physics*, Vol.37, pp. 3195 - 3203.
- Litchinitser N. M.; Abeeluck A. K.; Headley C.; Eggleton B. J. (2002). Antiresonant reflecting photonic crystal optical waveguides. *Optics Letters*, Vol.27, pp. 1592 - 1594.
- Lord Rayleigh (1907). Note on the remarkable case of diffraction spectra described by Prof. Wood. *Philosophical magazine Series 6*, Vol.14, pp. 60 - 65.
- Marcatili E. A. & Schmeltzer R. A. (1964). Hollow metallic and dielectric waveguides for long distance optical transmission and lasers. *The Bell system technical journal*, Vol. 43, pp. 1783 - 1809.
- Mashida H., Nishimura A., Ishikawa M., and Miyagi H. (1991). Low loss lead fluoride – coated square waveguides for CO₂ laser light transmission. *Electr. Letters*, Vol. 27, pp. 2068 - 2070.
- Miyagi, M., Kawakami, S. (1984). Design Theory of Dielectric-Coated Circular Metallic Waveguides for Infrared Transmission. *Journal of Lightwave Technology*, Vol.LT-2, No.2, pp.116-126.
- Miyagi, M., Hongo, A., Yoshizo, A. & Kawasami. S. (1983). Fabrication of germanium-coated nickel hollow waveguides for infrared transmission. *Appl. Phys. Letters*, Vol.43, No.5, pp.430-432.
- Morrow C. and Gu G. (1994). *Soc. Photo – Opt. Instrum. Eng.*, v. 2131, p. 18.
- Nishihara, H.; Inoue, T., Koyama, J. (1974). Low-loss parallel-plate waveguide at 10.6 μm. *Appl. Phys. Letters*, Vol.25, No.7, pp.391-393.
- Nubling, R.K., Harrington, J.A. (1996). Hollow-waveguide delivery systems for high-power, industrial CO₂ lasers. *Applied Optics*, Vol.34, No.3, pp. 372-380.
- Pearce, G.J., Pottage, J.M., Bird, D.M., Roberts, P.J., Knight, J.C., Russell, P.St.J. (2005). Hollow-core PCF for guidance in the mid to far infra-red, *Optics Express*, Vol.13, No.18., pp. 6937-6946.
- Pearce G. J.; Wiederhecker G. S.; Poulton C. G.; Burger S.; Russell P. St. J. (2007). Models for guidance in kagome structured hollow core photonic crystal fibres. *Optics Express*, Vol. 15, pp. 12680 - 12685.
- Pottage, J.M., Bird, D.M., Hedley, T.D., Birks, T.A., Knight, J.C., Russell, P.St.J. (2003). Robust photonic band gaps for hollow core guidance in PCF made from high index glass, *Optics Express*, Vol.11, No.22, pp.2854-2861.

- Pryamikov A. D.; Biriukov A. S.; Kosolapov A. F.; Plotnichenko V. G.; Semjonov S. L.; E. M. Dianov. (2011). Demonstration of a waveguide regime for a silica hollow core microstructured optical fiber with a negative curvature of the core boundary in the spectral region $> 3.5 \mu\text{m}$. *Optics Express*, Vol.19, pp. 1441 - 1448.
- Pryamikov A.D., to be prepared.
- Roberts P. J., Couny F., Sabert H., Mangan B. J., Williams D. P., Farr L., Mason M. W., Tomlinson A., Birks A., Knight J.C., Russell P. St. J. (2005). Ultimate low loss of hollow - core photonic crystal fibers. *Opt. Express*, Vol. 13, pp. 236 - 244.
- Roberts, P.J., Williams, D.P., Mangan, B.J., Sabert, H., Couny, F., Wadsworth, W.J., Birks, T.A., Knight, J.C., Russell, P.St.J. (2005). Realizing low loss air core photonic crystal fibers by exploiting an antiresonant core surround, *Optics Express*, Vol.13, No.20, pp. 8277-8285.
- Saitoh K.; Mortensen N. A.; Koshiba M. (2004). Air core photonic band gap fibers: the impact of surface modes. *Optics Express*, Vol. 12, pp. 394 - 400.
- Shaw, L.B., Sanghera, J.S., Aggarwal, I.D., Kung, F.H. (2003). As-S and As-Se based photonic band gap fiber for IR laser transmission, *Optics Express*, Vol.11, No.25, pp.3455-3460.
- Shephard, J.D., MacPherson, W.N., Maier, R.R.J., Jones, J.D.C., Hand, D.P., Mohebbi, M., George, A.K., Roberts, P.J., Knight, J.C. (2005). Single-mode mid-IR guidance in a hollow-core photonic crystal fiber, *Optics Express*, Vol.13, No.18, pp.7139-7144.
- Smith C. M.; Venkataraman N.; Gallagher M. T.; Muller D.; West J. A.; Borrelli N. F.; Allan D. C.; Koch K. W. (2003). Low - loss hollow - core silica/air photonic bandgap fibre. *Nature*, Vol.424, pp. 657 - 659.
- Skorobogatiy M.&Yang J. (2009). *Fundamentals of Photonic Crystal Guiding*, Cambridge University Press, ISBN - 10: 0521513286.
- Snyder A. W. (1971). Continuous mode spectrum of a circular dielectric rod. *IEEE Transactions on Microwave Theory and Techniques*, Vol.MTT - 19, pp. 720 - 727.
- Steinvurzel P.; de Sterke C. M.; Steel M. J.; Kuhlmeiy B. T.; Eggleton B. J. (2006). Single scatterer Fano resonances in solid core photonic band gap fibers. *Optics Express*, Vol.14, pp. 8797 - 8811.
- Temelkuran B.; Hart S. D.; Benoit G.; Joannopoulos J. D.; Fink Y. (2002). Wavelength - scalable hollow optical fibres with large photonic bandgap for CO₂ laser transmission. *Nature*, Vol. 420, pp. 650 - 653.
- Wait J. R. (1955). Scattering of a plane wave from a circular dielectric cylinder at oblique incidence. *Canadian Journal of Physics*, Vol. 33, pp. 189 - 195.
- Wang Y.; Couny F.; Roberts P. J.; Benabid F. (2011). Low loss broadband transmission in hypocycloid - core kagome hollow core photonic crystal fiber. *Optics Letters*, Vol. 36, pp. 669 - 671.
- West, J.A., Smith, C.M., Borrelli, N.F., Allen, D.C., Koch, K.W. (2004). Surface modes in air-core photonic band-gap fibers, *Optics Express*, Vol.12, No.8, pp.1485-1491.
- White T. P.; Kuhlmeiy B. T.; McPhedran R. C.; Maystre D.; Renversez G.; de Sterke C. M.; Botten L. C. (2002). Multipole method for microstructured optical fibers. *Journal of the Optical Society of America B*, Vol.19, pp. 2322 - 2330.
- Wood R. W. (1902). On remarkable case of uneven distribution of light in a diffraction grating spectrum, *Philosophical magazine Series 6*, Vol. 4, pp. 396 - 402.

- Vincetti L.; Setti V. (2010). Waveguide mechanism in tube lattice fibers. *Optics Express*, Vol.18, pp. 23133 - 23146.
- Yeh P.; Yariv A.; Marom E. J. (1978). Theory of Bragg fiber. *Journal of the Optical Society of America*, Vol.68, pp. 1196 - 1201.

IntechOpen

IntechOpen



CO2 Laser - Optimisation and Application

Edited by Dr. Dan C. Dumitras

ISBN 978-953-51-0351-6

Hard cover, 436 pages

Publisher InTech

Published online 21, March, 2012

Published in print edition March, 2012

The present book includes several contributions aiming a deeper understanding of the basic processes in the operation of CO₂ lasers (lasing on non-traditional bands, frequency stabilization, photoacoustic spectroscopy) and achievement of new systems (CO₂ lasers generating ultrashort pulses or high average power, lasers based on diffusion cooled V-fold geometry, transmission of IR radiation through hollow core microstructured fibers). The second part of the book is dedicated to applications in material processing (heat treatment, welding, synthesis of new materials, micro fluidics) and in medicine (clinical applications, dentistry, non-ablative therapy, acceleration of protons for cancer treatment).

How to reference

In order to correctly reference this scholarly work, feel free to copy and paste the following:

A. D. Pryamikov, A. F. Kosolapov, V. G. Plotnichenko and E. M. Dianov (2012). Transmission of CO₂ Laser Radiation Through Glass Hollow Core Microstructured Fibers, CO₂ Laser - Optimisation and Application, Dr. Dan C. Dumitras (Ed.), ISBN: 978-953-51-0351-6, InTech, Available from:
<http://www.intechopen.com/books/co2-laser-optimisation-and-application/transmission-of-co2-laser-radiation-through-glass-hollow-core-microstructured-fibers>

INTECH
open science | open minds

InTech Europe

University Campus STeP Ri
Slavka Krautzeka 83/A
51000 Rijeka, Croatia
Phone: +385 (51) 770 447
Fax: +385 (51) 686 166
www.intechopen.com

InTech China

Unit 405, Office Block, Hotel Equatorial Shanghai
No.65, Yan An Road (West), Shanghai, 200040, China
中国上海市延安西路65号上海国际贵都大饭店办公楼405单元
Phone: +86-21-62489820
Fax: +86-21-62489821

© 2012 The Author(s). Licensee IntechOpen. This is an open access article distributed under the terms of the [Creative Commons Attribution 3.0 License](#), which permits unrestricted use, distribution, and reproduction in any medium, provided the original work is properly cited.

IntechOpen

IntechOpen